Draft version December 24, 2014
Preprint typeset using LaTeX style emulateapj v. 04/17/13

RADIO PROPERTIES OF YOUNG PROTOSTARS IN THE CENTRAL FILAMENT OF THE SERPENS SOUTH INFRARED DARK CLOUD

Authors

ABSTRACT

We present 4.14 and 6.31 centimeter continuum observations of the Serpens South protocluster with the Karl G. Jansky Very Large Array in its C configuration. Our focus is a 3.5' x 3.5' area around the central filament. We detect roughly 18 sources, 10 of which are probably protostellar in nature. We characterize the radio emission and put it in context with 2MASS, Spitzer and Herschel data from the region. We compare our radio sources to the known centimeter vs. bolometric luminosity relationship. With our relatively short integration time and weak detection of many more possible radio sources, we speculate that longer, higher resolution radio measurements of the region would yield confident detections of many more protostars at centimeter wavelengths. [Not finished...]

1. INTRODUCTION

Serpens South is a young stellar cluster that is a part of the broader Aquila Rift extinction feature. It lies south of the Serpens Main cloud and is just West of the bright W40 HII region. Discovered in 2008 by Gutermuth et al. (2008) as a part of the Spitzer Space Telescope's Gould Belt Legacy Survey, Serpens South has been found to harbor an unusually high ratio of Class I to Class II protostars suggesting it is in a very early phase of cluster formation.

Since its discovery, it has become the center of a wide range of scholarship. This has consisted of near, mid and far infrared mappings with Spitzer and Herschel tracing heated dust around protostars (Gutermuth et al. 2008; Bontemps et al. 2010), millimeter mappings tracing cold dust (Maury et al. 2011), near infrared polarimetry revealing the importance of global magnetic fields in the cluster's formation history (Sugitani et al. 2011), molecular outflows studies (Nakamura et al. 2011; Teixeira et al. 2012), and a wealth of spectral line surveys probing filamentary infall (Kirk et al. 2013; Friesen et al. 2013; Tanaka et al. 2013; Fernández-López et al. 2014; Nakamura & Li 2014). X-ray studies of Serpens South have yet to be published. Presently only one radio study of Serpens South has been conducted, which used the Karl G. Jansky Very Large Array (VLA) in its A configuration in 2011 (Ortiz-Leon et al. in prep).

Early radio studies of protostars found an excess of radio emission compared to the Lyman-Alpha continuum drop off expected from a normal ZAMS star. Theory and observations have best explained protostellar radio emission as having two components, thermal and non-thermal. Thermal radio emission is generally assumed to be free-free emission created from an HII region. High mass protostars have a high enough internal luminosity to support a compact or ultra-compact HII region, however, low mass protostars do not. Free-free emission around low-mass protostars arises from shocks at the base of protostellar jets that shock the surrounding envelope material. Non-thermal emission around young (Class 0 and I), low and high mass protostars is still not clearly understood; it is thought to come from gyrosynchrotron emission created by stellar magnetic fields. (The gyrosynchrotron can also be magnetic reconnection events in their coronae I believe, check some of the recent Goulds Belt distance papers for their explanations.)

The VLA has been a proven tool for detecting radio emission around protostars since the early 1990s (e.g., Curiel et al. 1989; Anglada et al. 1998; Reipurth et al. 1999; Beltrán et al. 2001; Eiroa et al. 2005; Shirley et al. 2007; Rodríguez et al. 2010; Dzib et al. 2013). With the goal of locating embedded protostars in the Serpens South protocluster, we carried out VLA observations of Serpens South's central filament at 4.1 and 6.3 centimeters. In §2 we present our observations. In §3 we present our results. In §4 we discuss the implications of our study and in §5 we summarize our results.

1.1. *Distance to Serpens South*

The distances to Serpens South, W40 and the Serpens Main cloud are not agreed upon in the literature. When Serpens South was discovered in 2008, a distance of 260 pc ± 37 pc was adopted based on evidence that its LSR velocities matched LSR velocities of the Serpens Main cloud, which was then thought to be a part of the larger Aquila Rift extinction feature estimated to lie at 260 pc (Straižys et al. 2003). However, VLBA parallax measurements conducted in 2010 have established the distance to the Serpens Main cloud as 429 ± 2 pc (Dzib et al. 2011), meaning that Serpens Main is distinct from the the Aquila Rift if Aquila is to have a distance of 260 pc.

Gutermuth et al. (2008) also argued that Serpens South lies in front of W40, claiming that it is seen in absorption against emission from W40. If we are to follow the initial LSR velocity analysis by Gutermuth et al. (2008), we would equate Serpens South to Serpens Main and say Serpens South lies at approximately 429 pc, while W40 lies further away. Indeed, recent radio and x-ray studies adopt a distance of 600 pc to W40, although they admit the distance is poorly constrained (Kuhn et al. 2010; Rodríguez et al. 2010). Here, we adopt a distance of 429 pc for Serpens South, although we comment on how a 260 pc distance estimate would change our analysis.

2. OBSERVATIONS

We observed Serpens South on July 2, 2013, for 1 hour with the VLA in its C array configuration. In order to derive a spectral index, we split our C band observation

TABLE 1
VLA Image Properties

Wavelength (cm)	Beam Size[a] (arcsec x arcsec)	Position Angle (degrees)	Image RMS (μJy beam^{-1})
6.31	4.8 x 3.9	13.4	11.1
4.14	3.2 x 2.5	12.7	8.5

[a] Deconvolved with robust weighting, *robust*=0.5 (Briggs 1995).

into two subbands centered at 4.75 GHz (6.31 cm) and 7.25 GHz (4.14 cm) with a bandwidths of 1.024 GHz. At 4.75 and 7.25 GHz, our images had primary beam diameters of 9.5 and 6.2 arcminutes respectively. Our observation focused on a 3.5 arcmin x 3.5 arcmin region around Serpens South's central filament, with a phase center positioned at α(J2000) = $18^{h}30^{m}05.00^{s}$, δ(J2000) = $-02°02'30.0''$ (Figure 1). During our hour-long observation, we switched from Serpens South to J1804 + 0101 every 10 minutes for gain calibrations.

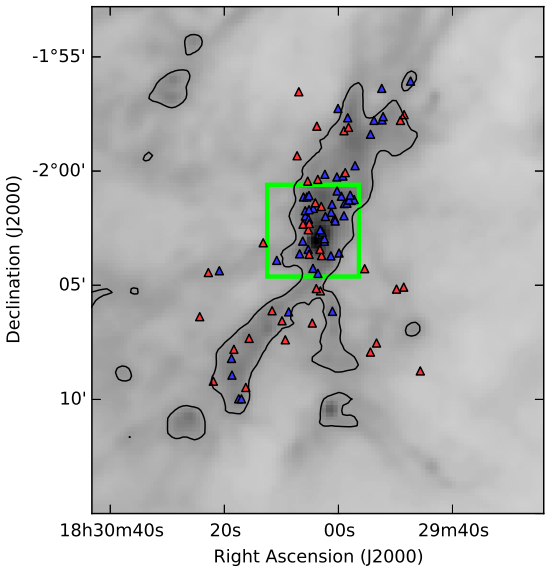

Fig. 1.— Herschel SPIRE 350 μm greyscale image of Serpens South outlining its filamentary structure. Blue and red triangles indicate Spitzer identified Class I and Class II protostars respectively. The green box indicates our region of interest with the VLA. The black contour intensity level is set at 365 mJy/sr.

We manually flagged, calibrated and imaged our data with standard procedures using Common Astronomy Software Applications (CASA) 4.1.0. We used J1331+305 (3C286) as a flux and bandpass calibrator, and J1804+0101 as a gain and phase calibrator ($S_{6.31cm}$ = 0.70 ± 0.02 Jy, $S_{4.14cm}$ = 0.66 ± 0.02 Jy). We deconvolved the Stokes I images with the Cotton-Schwab algorithm (Schwab 1984) using the CLEAN method (Högbom 1974; Clark 1980). We experimented with natural, robust and uniform weighting, and found the best compromise between noise level and source resolution using robust weighting (Briggs 1995), with the *robust* parameter set to 0.5. The synthesized beam sizes and RMS values for our two images are detailed in Table 1. We performed a primary beam correction on our images by convolving the CLEANed images with the array's modeled flux response.

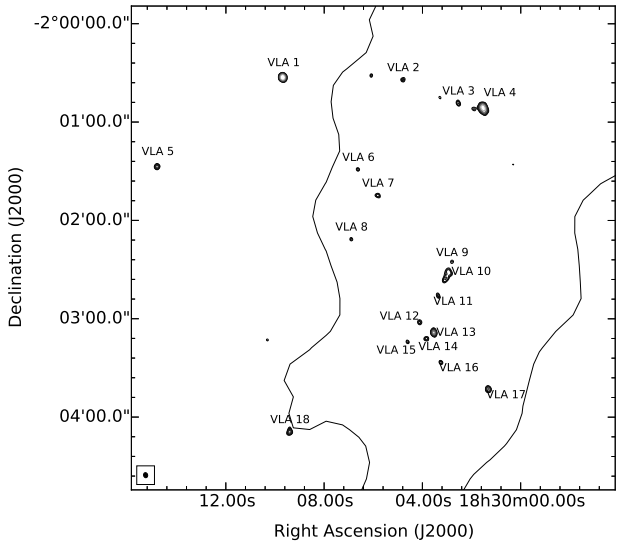

Fig. 2.— Serpens South's central filament at 4.1 cm, focused in on the green box from Figure 1. Radio contours start at 4σ and end at 50σ. The loose black contour is the same SPIRE 350 μm contour found in Figure 1.

3. RESULTS

3.1. *Radio Source Selection*

Out of the 50+ Spitzer identified Class I and II YSOs located in and around Serpens South's central filament, we detect 18 radio sources at our sensitivity level. In choosing our sources, we restricted ourselves to a circular region centered on our phase center extending out to 50% of the primary beam response. We chose our sources based on their appearance and strength in both our 4.1 and 6.3 cm images, their spatial proximity to infrared associations, and by referencing a source extracted sample using Sextractor (Bertin & Arnouts 1996). We only took sources that had at least a 4σ detection in the 4.1 cm image. We note that we found ∼6 sources at the 2σ level that aligned within 2 arcsecond of infrared associations, however, we do not consider them strong detections and do not include them in our final source list. Further observations with higher sensitivity will likely be able to confidently detect these protostellar radio sources.

We used CASA's IMFIT function to fit 2D gaussians to our chosen radio sources. For strong and relatively isolated sources, we can reasonably rely on the 2D gaussian integrated flux densities. For somewhat blended sources, such as VLA 9 and 14, manually-calculated peak fluxes are likely more reliable for spectral index calculations. Integrated flux errors were calculated by adding in quadrature the flux error output from IMFIT with an assumed 5% systematic flux calibration error. Peak flux errors were calculated by adding in quadrature the relative error of the image RMS with an assumed 5% systematic flux calibration error.

We cross-referenced our radio source positions with the 2MASS catalogue, and ran source extractions over the four IRAC bands of Spitzer, the 24 μm MIPS band on Spitzer, and the 70 μm PACS band on Herschel. We used a 2 arcsecond maximum matching tolerance for these ex-

TABLE 2
RADIO PROPERTIES OF VLA SOURCES

Source	RA[a] (J2000)	Decl.[a] (J2000)	$S^{int}_{6.3cm}$ [b] (μJy)	$S^{peak}_{6.3cm}$ (μJy beam^{-1})	$S^{int}_{4.1cm}$ (μJy)	$S^{peak}_{4.1cm}$ (μJy beam^{-1})	α^{int}_{radio}	α^{peak}_{radio}	Class[e]
VLA_1	18 30 09.68	-02 00 32.8	749 ± 42	718	844 ± 43	794	0.28 ± 0.08	0.24 ± 0.07	Extragal.?
VLA_2	18 30 04.79	-02 00 34.1	177 ± 5	138	87 ± 8	72	-1.67 ± 0.1	-1.55 ± 0.16	Extragal.
VLA_3	18 30 02.55	-02 00 48.5	140 ± 6	99	116 ± 12	87	-0.46 ± 0.11	-0.3 ± 0.16	Extragal.
VLA_4	18 30 01.53	-02 00 51.6	1663 ± 50	1178	946 ± 55	515	-1.33 ± 0.07	-1.96 ± 0.07	Extragal.
VLA_5	18 30 14.79	-02 01 27.3	106 ± 12	95	167 ± 13	173	1.07 ± 0.14	1.41 ± 0.14	Extragal.?
VLA_6	18 30 06.62	-02 01 28.9	79 ± 3	61	33 ± 4	56	-2.04 ± 0.15	-0.22 ± 0.24	Extragal.
VLA_7	18 30 05.81	-02 01 44.9	48 ± 8	40	84 ± 8	63	1.29 ± 0.2	1.08 ± 0.31	Class I
VLA_8	18 30 06.89	-02 02 11.5	39 ± 5	46	50 ± 6	50	0.55 ± 0.19	0.18 ± 0.3	Extragal.?
VLA_9	18 30 02.80	-02 02 25.3	66 ± 3	50	60 ± 3	44	-0.22 ± 0.07	-0.31 ± 0.3	Class 0*?
VLA_10	18 30 02.95	-02 02 32.2	287 ± 14	119	260 ± 21	73	-0.23 ± 0.1	-1.15 ± 0.16	Unknown
VLA_11	18 30 03.36	-02 02 45.8	38 ± 6	36	73 ± 5	58	1.5 ± 0.17	1.14 ± 0.34	Class 0
VLA_12	18 30 04.11	-02 03 02.1	30 ± 8	24	79 ± 4	58	2.31 ± 0.27	2.06 ± 0.48	Class 0
VLA_13	18 30 03.54	-02 03 08.4	186 ± 11	178	231 ± 12	227	0.51 ± 0.08	0.58 ± 0.1	Class 0
VLA_14	18 30 03.84	-02 03 12.2	31 ± 4	37	83 ± 4	61	2.29 ± 0.15	1.19 ± 0.33	Class 0*
VLA_15	18 30 04.60	-02 03 14.1	68 ± 2	52	49 ± 4	51	-0.74 ± 0.1	-0.08 ± 0.28	Extragal.
VLA_16	18 30 03.25	-02 03 26.6	63 ± 3	58	55 ± 3	65	-0.28 ± 0.08	0.27 ± 0.24	Class II
VLA_17	18 30 01.32	-02 03 42.9	146 ± 8	135	161 ± 9	167	0.22 ± 0.08	0.5 ± 0.12	Class I
VLA_18	18 30 09.40	-02 04 08.8	170 ± 9	182	167 ± 13	134	-0.04 ± 0.1	-0.71 ± 0.11	Extragal.?

[a] Centers of 2D gaussian fits for sources in 4.1 cm map, quoted in J2000 coordinates.
[b] Flux values from images deconvolved with Briggs weighting, *robust*=0.5 (Briggs 1995).
[c] Spectral index of integrated flux from 6.3 to 4.1 cm, see section 3 for details on calculation.
[d] Spectral index of peak flux from 6.3 to 4.1 cm.
[e] Classification of source. Unless otherwise noted, Class 0 classifications come from Herschel (Bontemps et al. 2010) and Class I & II from Spitzer (Gutermuth et al. 2008). (?) denotes uncertainty. (*) denotes classified by this work.

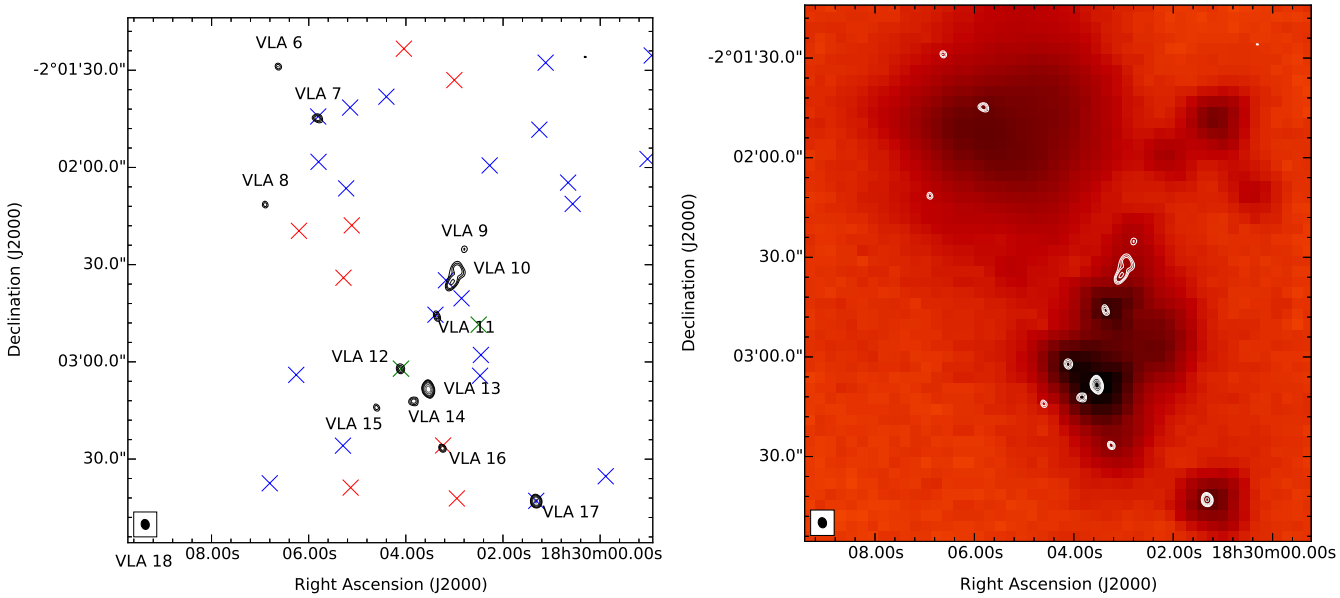

FIG. 3.— **Left**: Radio continuum of our sources VLA 6 to VLA 17 at 4.1 cm. Blue and red crosses correspond to Class I and II protostars, respectively, identified by Spitzer. Green crosses correspond to 1.2 mm dust peaks identified by IRAM. **Right**: Identical contours on the left but with a background PACS 70 μm image. The radio image beam size is shown to the lower-left.

tractions. Apertures and adopted corrections were consistent with the HOPS survey (Gutermuth et al. in prep).

Eight of our radio sources have at least one infrared source match from 1.25 μm to 70 μm, four of which spatially match a Spitzer identified Class I or II protostar within 1 arcsecond. A total of ten out of our 18 sources have signs that indicate they are protostellar in nature. One of our radio sources, VLA 12, matches a 1.2 mm source within 1 arcsecond identified by (Maury et al. 2011), which they identify as Class 0.

We can calculate the number of random background sources we would expect to find in our images. We use the formulation found in Shirley et al. (2007) and Dzib et al. (2013), who draw from radio studies done by Fomalont et al. (1991). The density of random background radio sources above a flux limit of S μJy at 6 cm is given by

$$n(>S) = 0.42 \pm 0.05 \left(\frac{S}{30\ \mu\text{Jy}}\right)^{-1.18\pm0.19} \quad \text{arcmin}^{-2}$$

Therefore, the total number of sources with flux S greater than 30 μJy at 6 cm is 0.42 arcmin^{-2}. This leads to a 0.7% chance that a background source falls inside a 4.8 x 3.9 arcsec synthesized beam centered on a compact radio source. It also gives us on average $\sim 6 \pm 1$ background sources within our 3.5' x 3.5' region of interest above a 3σ level. We find roughly 5 to 8 sources that we identify as extragalactic, which is at worst within 2 standard deviations from the expectation.

3.2. *Spectral Indices*

At radio wavelengths, the spectral index is defined as

$$\alpha_{\text{radio}} = \frac{\ln(S_{\lambda_1}/S_{\lambda_2})}{\ln(\lambda_2/\lambda_1)} \quad (1)$$

where $\lambda_2 > \lambda_1$ (Shirley et al. 2007). Note that we have defined S_λ in terms of a flux density (e.g. Jansky) and not a flux (e.g. λS_λ or νS_ν). Flat radio spectral indices ($\alpha > -0.1$) are generally indicative of optically thin free-free emission, while rising indices ($\alpha \sim 2.0$) are representative of optically thick free-free emission (Anglada et al. 1998).

3.3. *Radio Source Classifications*

Extragalactic Sources — VLA 2, 3, 4, 6, and 15 are very likely extragalactic in nature. They have no visible associations from 1μm to 70μm and have negative radio spectral indices indicative of non-thermal synchrotron emission typical of a galaxy's radio spectrum.

Unclear Sources — While VLA 1 and 5 have no infrared, far-infrared or millimeter associations and are isolated from the filament, they have a flat or rising radio spectral indices suggesting optically thin or thick free-free emission respectively. Although galaxies can produce free-free emission from large HII clouds, the dominant component of a galaxy's radio emission output comes from non-thermal synchrotron emission with a declining spectrum. Moreover, in Dzib et al. (2013)'s study of 190 radio sources in the Ophiuchus star forming cloud, they didn't find a single extragalactic source with a radio spectral index larger than $\sim$0. Nonetheless, we tentatively classify these sources as extragalactic due to their lack of any association at shorter wavelengths.

VLA 18 is spatially distinct from the filament but has a flat radio spectral index and actually has three very weak infrared associations at 3.6, 4.5 and 5.8 μm. However, we speculate that these associations are coincidental due to their odd linear behavior, and tentatively classify VLA 18 as extragalactic.

We are unsure as to the nature of VLA 10. We treat the whole elongated structure as one source. At our higher resolution 4.1 cm image, we can resolve two distinct emission components that are blended at our lower resolution 6.3 cm image (Figure 5). We cannot confidently rely on our gaussian fitted fluxes due to the morphology of the source. For VLA 10's peak flux, we used the Northern structure in the 4.1 cm map. Although our measured peak fluxes are highly uncertain due to confusion at 6.3 cm, VLA 10's peak flux derived spectral index is strongly negative suggesting non-thermal emission and an extragalactic classification. However, VLA 10's Southern structure is also within 2 arcseconds of a Spitzer identified Class I source. This raises the possibility that the Northern structure is a background source while the Southern structure is a Class I protostellar radio source.

Another possibility is that VLA 10 is representative of an outflow shock emanating from either the Southern VLA 10 structure or from sources VLA 11 or 9. An H_2 study conducted by Teixeira et al. (2012), however, labeled VLA 11 as an outflow source with a jet running from North-East to South-West, almost perpendicular to the direction necessary for it to be an outflow source powering VLA 10's emission. Further evidence that would support a non-extragalactic classification of both the South and North structures of VLA 10 is the fact that the dust seen at and longward of 70 μm neatly fits around VLA 10's elongated morphology, as seen in Figure 3.

Lastly, the fact that VLA 10 is elongated anti-parallel to the synthesized beam's natural eccentricity emphasizes the fact that the morphology is true source structure and not artificial. Higher resolution observations should be able to spatially separate and resolve the individual emission components and better determine the nature behind its radio signal.

Protostellar Sources — The remainder of our sources, VLA 7, 9, 11, 12, 13, 14, 16 and 17, are likely protostellar in nature. VLA 7, 11, 12, 13, 16, and 17 are associated with Spitzer and Herschel identified Class 0, I and II protostars. All sources have either flat or rising radio spectral indices indicative of optically thin or thick free-free emission expected from an ionized plasma created by protostellar processes.

VLA 7 and 17 correspond to Spitzer Class I sources and have an average radio spectral index of 0.8 ± 0.2. VLA 16 is our only radio source associated with a Spitzer Class II protostar. Its peak flux-derived spectral index is likely more reliable than its integrated flux-derived spectral index due to weak spurious signal in close proximity at 6.3 cm.

While the infrared source associated with VLA 11 was initially classified as Class I with Spitzer data, it was later classified as Class 0 with Herschel images (Bontemps et al. 2010). We report a confident detection of compact radio emission at both 6.3 and 4.1 cm with a rising spectrum suggesting optically thick free-free emis-

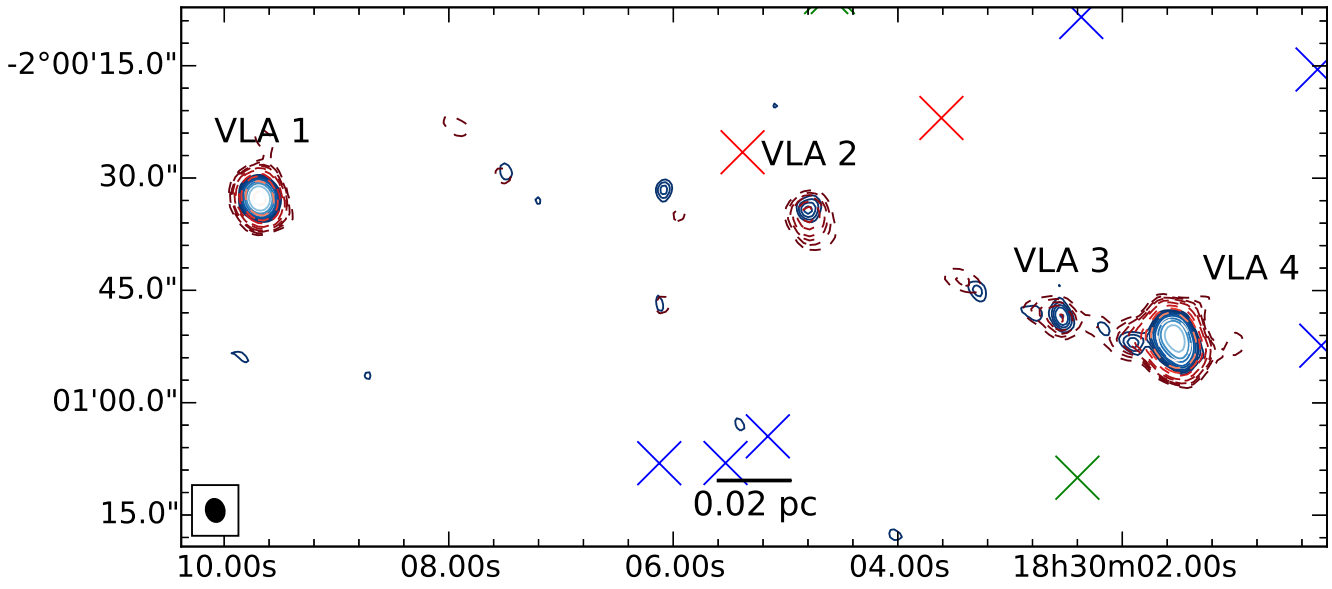

FIG. 4.—

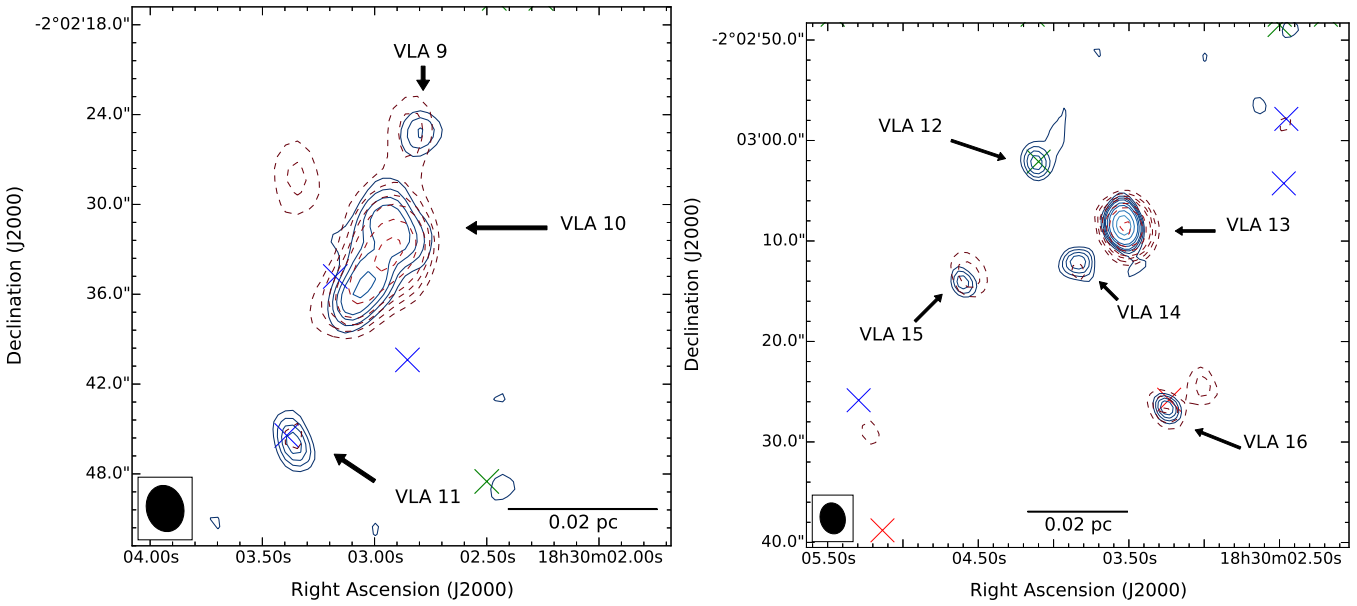

FIG. 5.— **Left**: Zoom-in of the elongated VLA 10 source. Blue solid and red dashed contours correspond to 4.1 and 6.3 cm images, respectively, and start at the 4σ level. The lower-left beam is the 4.1 cm beam size. Blue crosses represent Spitzer identified Class I sources. **Right**: Zoom-in of VLA 12 and surrounding sources. Blue solid contour is 4.1 cm data and red dashed contour is 6.3 cm data. Both radio contours start at their respective 3σ level. Blue crosses are Spitzer identified Class I sources. Green cross is IRAM 1.2 mm identified Class 0 source.

sion, which agrees with the notion that it is perhaps more embedded than previously thought.

VLA 12 is not visible short-ward of 24 microns. It is, however, the peak structure of diffuse 1.2 mm emission tracing cold dust and was therefore classified as a Class 0 source (Maury et al. 2011). This classification used a 25 arcsecond FWHM fit, which encompassed the infrared sources associated with VLA 13 and 14. Here, we confirm VLA 12's Class 0 classification with the detection of compact radio emission, which Andre et al. (2000) list as one of the qualifications for a Class 0 protostar.

For VLA 13, we find infrared associations on the IRAC 2, 3 and 4 bands but not on the IRAC 1 band at 3.6 μm. We report an infrared spectral index from 8 to 24 μm of $\sim$2.4, which, according to Lada (1987)'s classification scheme, would make it a Class I protostar. Herschel studies, however, classify it as a Class 0 source (Bontemps et al. 2010). While we classify it as Class 0, it may in fact be in a late Class 0 phase transitioning to a Class I protostar.

In far-infrared images from 24 to 250 μm, it is clear that VLA 14 lies within or around a gaseous envelope (Figure 9). However, because of the low resolution of the PACS and SPIRE images, we do not retrieve any source extractions within 2 arcseconds of its radio peak. Even in the MIPS 24 μm image, it is not seen as an individual

source but rather an extension of the emission structure from VLA 13 (Figure 9). This is likely why previous studies missed this source, and implies that if a compact source exists it is likely extremely young or extremely embedded. Here, we show that VLA 14 is a distinct radio source with a steeply rising radio spectral index of $\sim$ 1.2, revealing the presence of an embedded Class 0 protostar. The 5 arcsecond separation between VLA 13 and 14 corresponds to an angular separation of only 0.01 pc ($\sim$2,000 AU) if Serpens South lies at a distance of 429 pc away. However, VLA 13 could lie much further away from VLA 14 in 3D coordinates.

We also tentatively classify VLA 9 as another Class 0 source, although this is somewhat speculative. Like VLA 14, it has no strong infrared associations–although it does lie within 5 arcseconds of a weak infrared source. Also similar to VLA 14, VLA 9 is placed in a region of high protostellar density and falls in front of diffuse far-infrared emission. Its 6.3 cm emission does, however, begin to blend with VLA 10 at the 3σ level, raising the possibility that it is tied to the structure powering VLA 10's radio emission (Figure 5).

4. DISCUSSION

4.1. *Protostars in the Central Filament*

[Comment on how out of 50+ Spitzer identified Class I and II protostars and half a dozen Class 0 protostars identified by Herschel in our field of view, we only confidently detect $\sim$ 6, and weakly detect $\sim$ 11. Anything to be said about the clustering of the three Class 0 protostars in the center of our field of view? VLA 13 and 14 have an angular separation of only 0.01 pc, anything interesting we can say?]

4.2. *Sources of Outflow*

Early radio studies found that radio jet candidates are elongated in approximately the same direction as the large-scale outflow (**?**).

H_2 ν = 1–0 S(1) 2.122 μm line imaging conducted by Teixeira et al. (2012) showed that the infrared sources associated with VLA 11, 13 and 17 are sources driving large scale outflows. VLA 11 and 13's radio emission structures at 4.1 cm mildly reflect this, as they are slightly elongated in the proposed direction of outflow (Figure 5). VLA 17's morphology does not exceed the natural eccentricity of the beam. Future sub-arcsecond resolution observations will likely be able to resolve the radio-loud jets at the center of VLA 11 and 13.

Nakamura et al. (2011) carried out CO (J = 3–2) and HCO^+ (J = 4–3) observations towards Serpens South to map the broad-scale outflow from the central filament.

We can't directly correlate outflow and envelope mass properties due to blending of dust sources etc etc.

4.3. *The S_{radio} and L_{bol} Relationship*

– talk about anglada, beltran, shirley, scaife and others who have plotted Sradio vs. Lbol

– mention that we cannot easily derive Lbol estimates due to source blending

– talk about Kryukova and Dunham relationship, mention errors etc.

– present plots

4.4. *VeLLOs*

The internal luminosity $L_{\rm int}$ of a protostar is defined as the total luminosity from the protostar and its circumstellar disk if present. The bolometric luminosity of a source can then defined as $L_{\rm bol} = L_{\rm int} + L_{\rm ext}$, where the external luminosity comes from the heated protostellar envelope. It is estimated that $L_{\rm ext}$ contributes to $L_{\rm bol}$ on the order of 0.1 $L_\odot$ Dunham et al. (2008) developed a scaling law relating an embedded protostar's 70 μm flux to its internal luminosity $L_{\rm int}$.

5. CONCLUSIONS

present major conclusions

– new protostars, better estimates of protostellar positions

– weak detection of a few more protostars, no evident detection of many protostars

– highly clustered and fragmentation of gas/dust evident

– outflow elongation for two sources

– Sradio and Lbol relationship

– VeLLO

– point to future studies

REFERENCES

Andre, P., Ward-Thompson, D., & Barsony, M. 2000, Protostars and Planets IV, 59 [3.3]

Anglada, G., Villuendas, E., Estalella, R., et al. 1998, AJ, 116, 2953 [1, 3.2]

Beltrán, M. T., Estalella, R., Anglada, G., Rodríguez, L. F., & Torrelles, J. M. 2001, AJ, 121, 1556 [1]

Bertin, E., & Arnouts, S. 1996, A&AS, 117, 393 [3.1]

Bontemps, S., André, P., Könyves, V., et al. 2010, A&A, 518, L85 [1, 2, 3.3]

Briggs, D. S. 1995, dissertation, New Mexico Inst. of Mining and Technology [1, 2, 2]

Clark, B. G. 1980, A&A, 89, 377 [2]

Curiel, S., Rodriguez, L. F., Bohigas, J., et al. 1989, Astrophysical Letters and Communications, 27, 299 [1]

Dunham, M. M., Crapsi, A., Evans, II, N. J., et al. 2008, ApJS, 179, 249 [4.4]

Dzib, S., Loinard, L., Mioduszewski, A. J., et al. 2011, in Revista Mexicana de Astronomia y Astrofisica Conference Series, Vol. 40, Revista Mexicana de Astronomia y Astrofisica Conference Series, 231–232 [1.1]

Dzib, S. A., Loinard, L., Mioduszewski, A. J., et al. 2013, ApJ, 775, 63 [1, 3.1, 3.3]

Eiroa, C., Torrelles, J. M., Curiel, S., & Djupvik, A. A. 2005, AJ, 130, 643 [1]

Fernández-López, M., Arce, H. G., Looney, L., et al. 2014, ApJ, 790, L19 [1]

Fomalont, E. B., Windhorst, R. A., Kristian, J. A., & Kellerman, K. I. 1991, AJ, 102, 1258 [3.1]

Friesen, R. K., Medeiros, L., Schnee, S., et al. 2013, MNRAS, 436, 1513 [1]

Gutermuth, R. A., Bourke, T. L., Allen, L. E., et al. 2008, ApJ, 673, L151 [1, 1.1, 2]

Högbom, J. A. 1974, A&AS, 15, 417 [2]

Kirk, H., Myers, P. C., Bourke, T. L., et al. 2013, ApJ, 766, 115 [1]

Kryukova, E., Megeath, S. T., Gutermuth, R. A., et al. 2012, AJ, 144, 31 [11, 12]

Kuhn, M. A., Getman, K. V., Feigelson, E. D., et al. 2010, ApJ, 725, 2485 [1.1]

Lada, C. J. 1987, in IAU Symposium, Vol. 115, Star Forming Regions, ed. M. Peimbert & J. Jugaku, 1–17 [3.3]

Maury, A. J., André, P., Men'shchikov, A., Könyves, V., & Bontemps, S. 2011, A&A, 535, A77 [1, 3.1, 3.3]

Nakamura, F., & Li, Z.-Y. 2014, ApJ, 783, 115 [1]

Nakamura, F., Sugitani, K., Shimajiri, Y., et al. 2011, ApJ, 737, 56 [1, 4.2]
Reipurth, B., Rodríguez, L. F., & Chini, R. 1999, AJ, 118, 983 [1]
Rodríguez, L. F., Rodney, S. A., & Reipurth, B. 2010, AJ, 140, 968 [1, 1.1]
Schwab, F. R. 1984, AJ, 89, 1076 [2]
Shirley, Y. L., Claussen, M. J., Bourke, T. L., Young, C. H., & Blake, G. A. 2007, ApJ, 667, 329 [1, 3.1, 3.2, 11, 12]
Straižys, V., Černis, K., & Bartašiūtė, S. 2003, A&A, 405, 585 [1.1]
Sugitani, K., Nakamura, F., Watanabe, M., et al. 2011, ApJ, 734, 63 [1]
Tanaka, T., Nakamura, F., Awazu, Y., et al. 2013, ApJ, 778, 34 [1]
Teixeira, G. D. C., Kumar, M. S. N., Bachiller, R., & Grave, J. M. C. 2012, A&A, 543, A51 [1, 3.3, 4.2]

APPENDIX

Questions I Still Need Answers To:

– Is it possible that VLA 2, 3 and 4 are all apart of a radio-loud extragalactic jet?

– Given the size of the beam and the size of VLA 1 and 4, should they be considered "resolved" ?

– Does optically thick thermal radio emission ($\alpha_{radio} > 1.0$) mean that the source is "embedded"? In other words, can a protostellar source still be considered "embedded" in the sense that it is invisible at IRAC wavelengths, but have a radio spectral index indicative of optically thin thermal emission ($\alpha_{radio} \sim 0$)?

– Is it even physically possible for VLA 10 to be a radio galaxy outflow source? In other words, is a 10 arcsecond angular extent on the size scale of typical radio galaxy jets?

– Can we get a table of Herschel protostars from Bontemps et al. 2010? Reason being is because I want to say if protostars have previously been detected or not.

– Are my classifications okay? Specifically, VLA 1, 5, 8, 9, 10 and 18?

– What does MIPS 24 μm emission trace around protostars, heated dust from disk?

– Can we say anything about the fact that out of 50+ Spitzer identified Class I and II protostars, only ∼6 show strong radio emission? What is up with that? Does this say anything about relative masses of these protostars (perhaps all mid-low mass?)

– Are the images to a high enough sensitivity to which we can say they are "deep" ?

– Title?

ADDITIONAL FIGURES

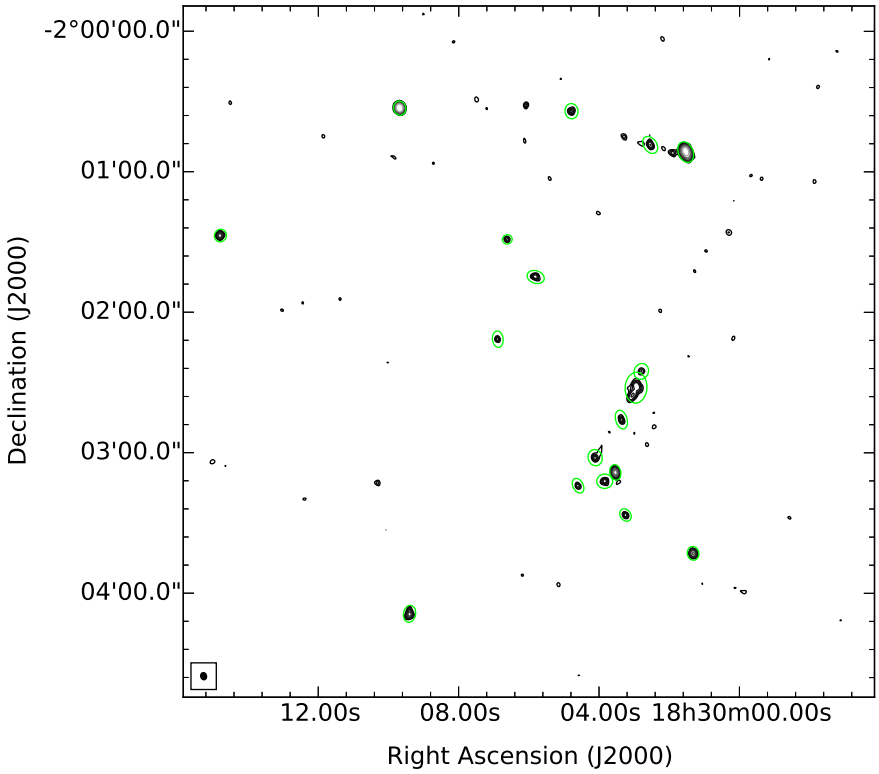

FIG. 6.— 4.1 cm map with 2D gaussian fits from CASA's IMFIT routine. Radio contours start at 3σ level.

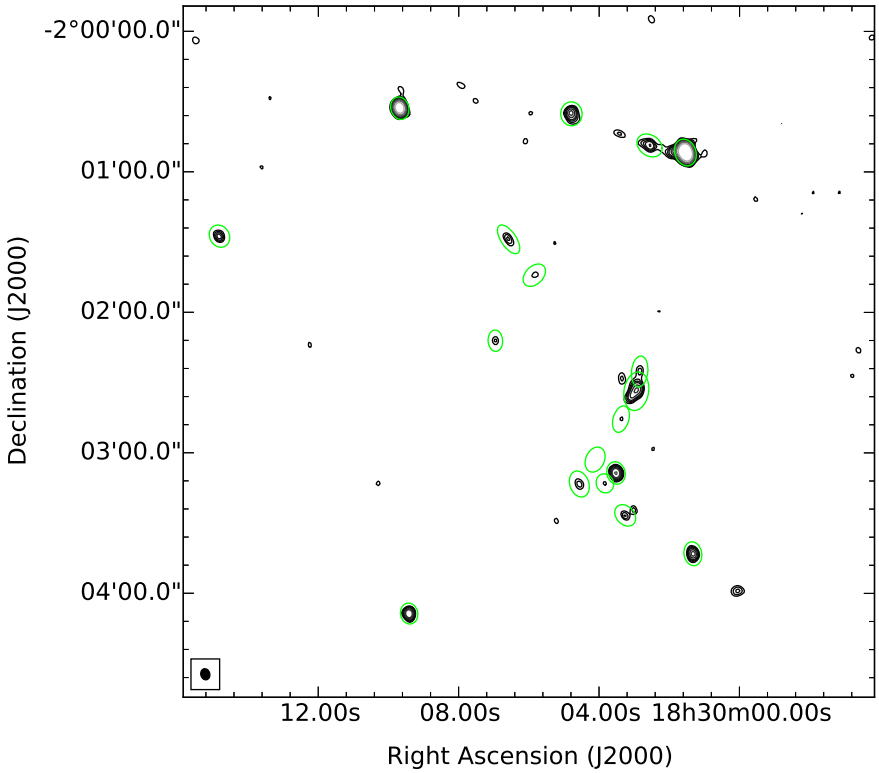

FIG. 7.— 6.3 cm map with 2D gaussian fits from CASA's IMFIT routine. Radio contours start at 3σ level.

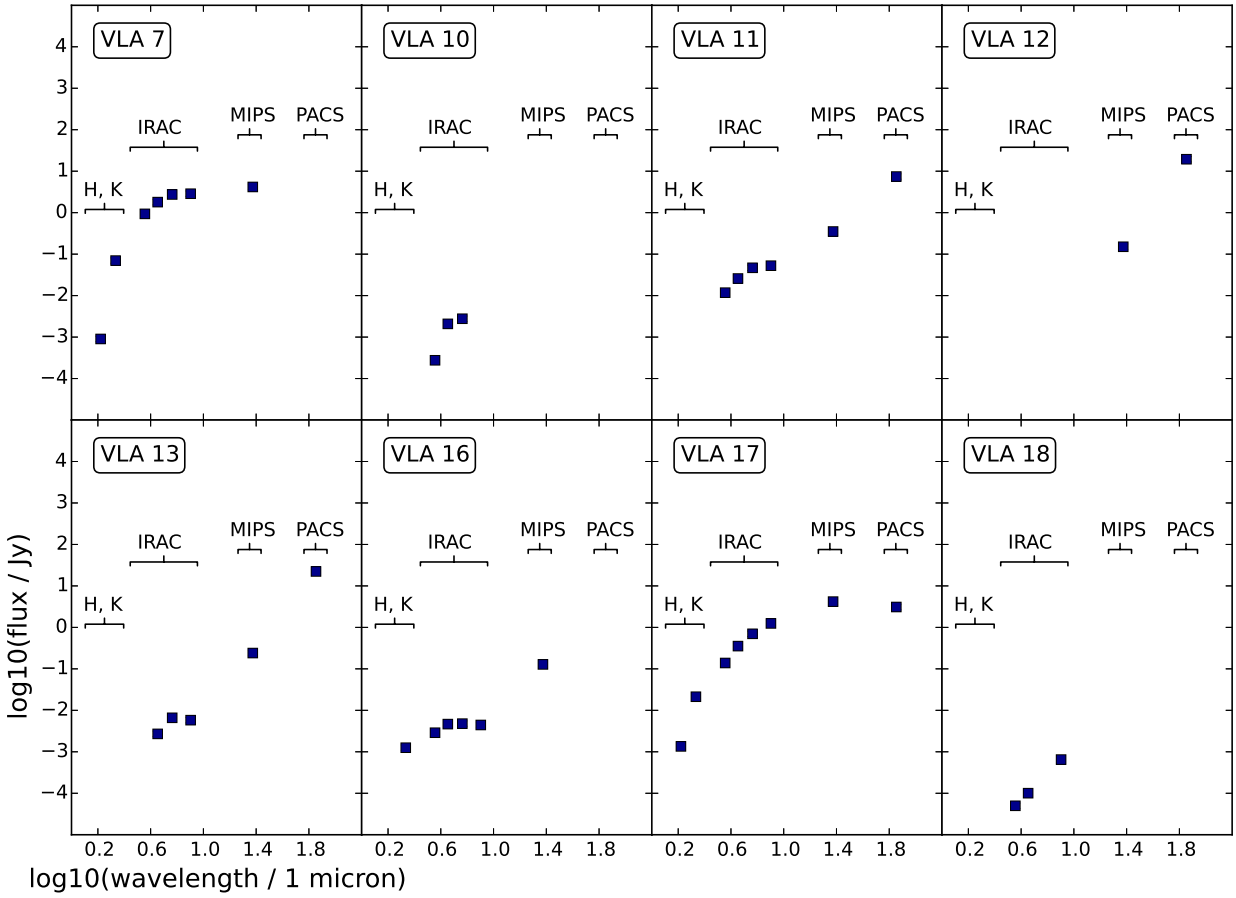

FIG. 8.— All VLA sources that have any catalogued infrared associations. Infrared bands are 2MASS H and K from 1.1 - 2.2 μm, IRAC 1, 2, 3 and 4 from 3.6 - 8.0 μm, MIPS 24μm and PACS 70μm.

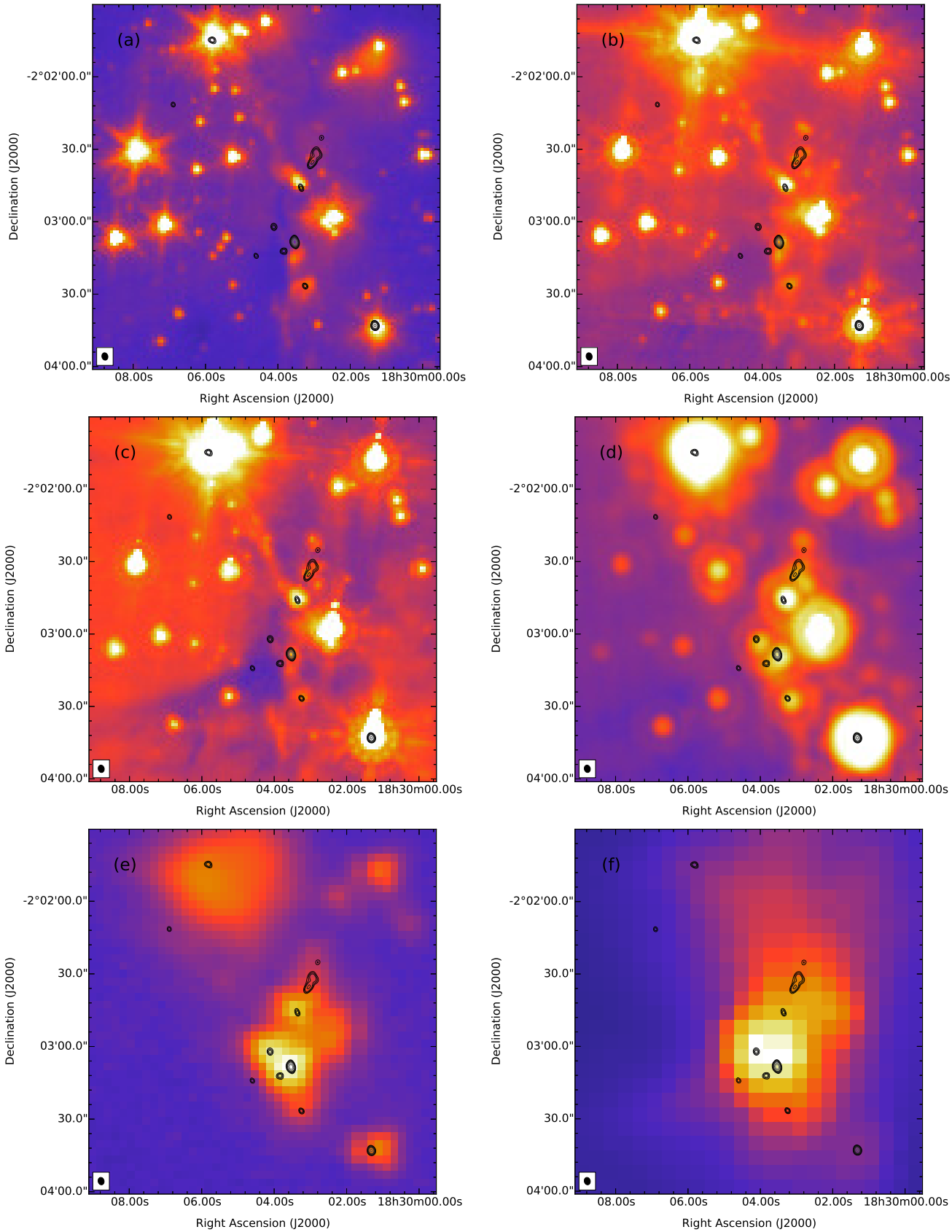

FIG. 9.— 4.1 cm radio contours plotted over infrared and far-infrared images ranging from 3.6 to 250 μm. Radio contours start at the 4σ level, with the deconvolved beam size shown at lower-left. **(a)** Spitzer IRAC 3.6 μm image. **(b)** Spitzer IRAC 5.8 μm image. **(c)** Spitzer IRAC 8.0 μm image. **(d)** Spitzer MIPS 24 μm image. **(e)** Herschel PACS 70 μm image. **(a)** Herschel SPIRE 250 μm image.

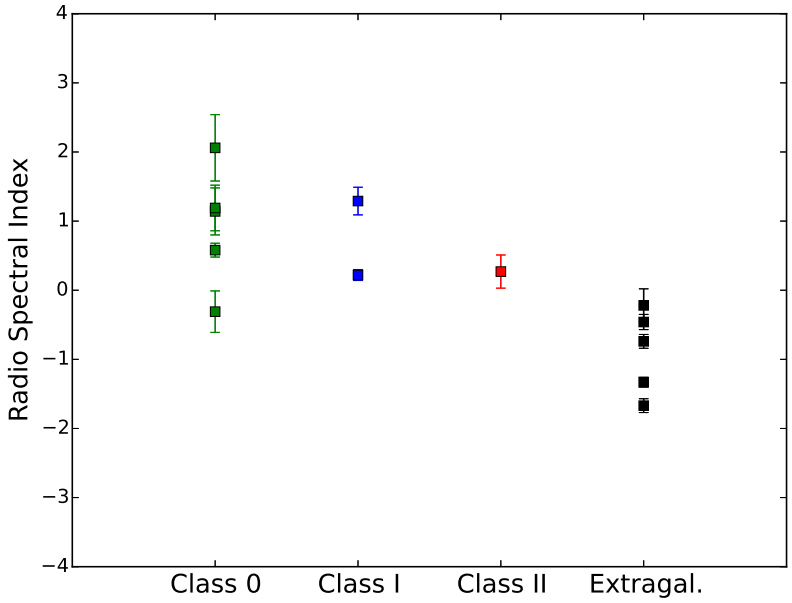

FIG. 10.— Radio spectral index of sources as a function of classification.

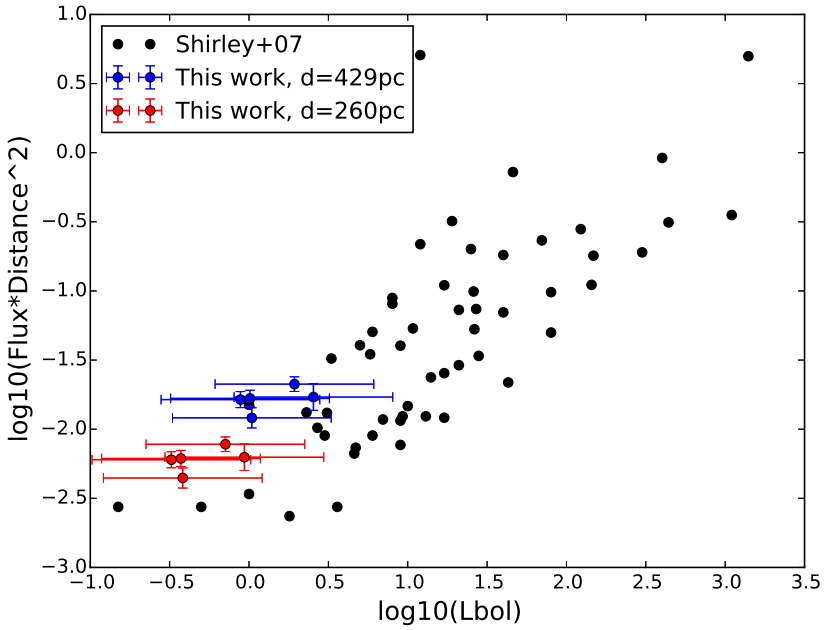

FIG. 11.— Figure 2 from Shirley et al. (2007) showing the 3.6 cm vs. Bolometric Luminosity correlation for protostars. Five of our protostellar sources are overlaid with a bolometric luminosities derived from a correlation that utilizes the protostars' mid-infrared luminosity (Kryukova et al. 2012). Figure reproduced from Shirley et al. (2007) with permission.

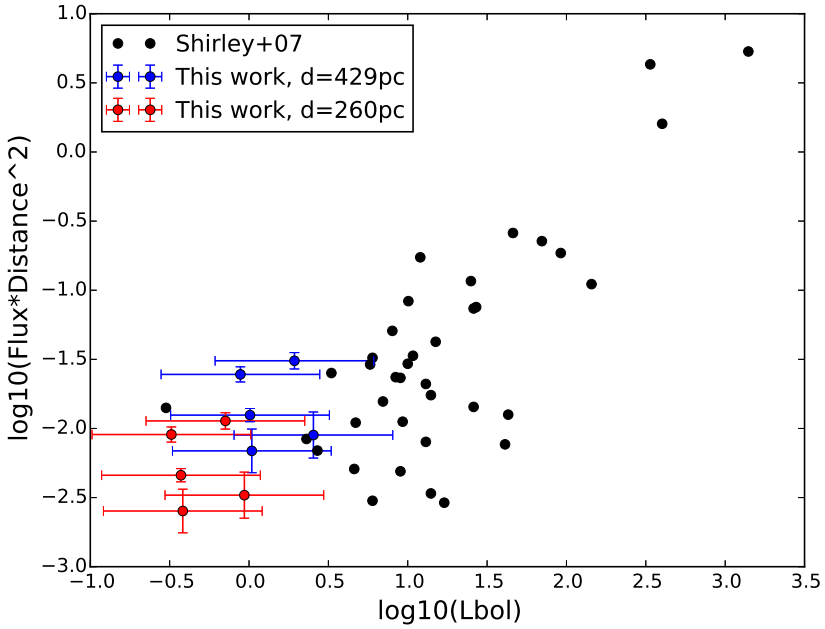

FIG. 12.— Figure 2 from Shirley et al. (2007) showing the 6.0 cm vs. Bolometric Luminosity correlation for protostars. Five of our protostellar sources are overlaid with a bolometric luminosities derived from a correlation that utilizes the protostars' mid-infrared luminosity (Kryukova et al. 2012). Figure reproduced from Shirley et al. (2007) with permission.